AGU ADVANCING EARTH AND SPACE SCIENCE

Geophysical Research Letters

RESEARCH LETTER
10.1029/2021GL094271

Delta Deposits on Mars: A Global Perspective

B. De Toffoli[1], A.-C. Plesa[1], E. Hauber[1], and D. Breuer[1]

[1]Institute of Planetary Research, DLR, Berlin, Germany

Key Points:

- We present an updated global catalog of deltas on Mars and characterize them in terms of their geomorphology
- Out of 161 deltas, 29 are located at the dichotomy boundary and only six can be used to investigate the presence of an oceanic shoreline
- Age and location of the six deltas are at odds with proposed shorelines; hence, deltas alone do not define a globally consistent water level

Supporting Information:

Supporting Information may be found in the online version of this article.

Correspondence to:

B. D. Toffoli,
Barbara.Detoffoli@dlr.de

Citation:

De Toffoli, B., Plesa, A.-C., Hauber, E., & Breuer, D. (2021). Delta deposits on Mars: A global perspective. *Geophysical Research Letters*, *48*, e2021GL094271. https://doi.org/10.1029/2021GL094271

Received 10 MAY 2021
Accepted 12 AUG 2021

Abstract Deltas have long been considered a constraining element to reconstruct the water level of an ancient ocean that may have once occupied the northern lowlands of Mars, and recently this hypothesis started to be challenged. We investigate this hypothesis and present a global inventory of fan-shaped features showing typical deltaic traits across the entire Martian surface. For each element, we provide descriptive details and classifications based on morphology, location, and relation with characterizing environmental features. In this catalog of 161 deltas, we identified only six having high potential to constrain an oceanic paleoshoreline. Nonetheless, age and location of these candidates display discrepancies with what was previously suggested from independent data sets about shoreline age and locations. Our analyses hence indicate that deltas alone are insufficient to delineate a globally consistent ancient oceanic shoreline, but they have the potential to locally constrain the water level both in space and time.

Plain Language Summary Deltas are sedimentary features generated by the deposition of fluid-carried sediments as a river flow enters a larger water body. These landforms have been observed on Mars and may have recorded the water level of the basin where they formed. In this study, we present a global distribution of deltas on Mars that we have characterized in terms of their geomorphology, location, and relation to their surroundings. A total of 161 deltas are included in this global catalog. Among them, only six deltas can be associated with the shoreline of a past Martian ocean. However, their estimated age and location are difficult to reconcile with previously proposed shorelines. This indicates that a global ocean level on Mars is difficult to constrain from the information provided by deltas alone. Instead, these features are more likely to indicate local-scale water levels during the Martian past.

1. Introduction

River deltas are landforms generated by deposition of fluid-carried sediments as the flow enters a slower-moving or stagnant water body. The presence of delta deposits on Mars has been thoroughly demonstrated for decades (e.g., Di Achille & Hynek, 2010; Nazari-Sharabian et al., 2020; Ori et al., 2000). Large scale mapping (Di Achille & Hynek, 2010; Di Biase et al., 2013; Hauber et al., 2013; Wilson et al., 2021) highlighted the presence of several delta fans mainly located at the dichotomy boundary. These features raised great interest due to their potential as indicators of water availability, habitable environments, and as favorable sedimentary settings for organic matter preservation and have been targeted as landing sites for robotic exploration (e.g., Goudge et al., 2017; Mangold et al., 2020; Summons et al., 2010). Furthermore, deltaic deposits have been investigated as potential evidence that a large ocean covered up to a third of the planet's surface occupying the northern lowlands of Mars (Di Achille & Hynek, 2010; Di Biase et al., 2013; Fawdon et al., 2018; Rivera-Hernández & Palucis, 2019). Overall, whether or not a large water body occupied a large portion of the northern hemisphere of Mars is still largely debated. Observations of possible shorelines from orbital images and valley networks terminating near these shorelines have been proposed as evidence supporting the ocean hypothesis (Clifford and Parker., 2001; Hynek et al., 2010; Ivanov et al., 2017; Perron et al., 2007), while arguments against it involved the hypothesis of a prolonged cold and dry climate that could not have sustained an ocean during the Martian past (Wordsworth et al., 2015) or a global paucity of water compared to the required amount to form such a widespread ocean in the first place (Carr & Head, 2015).

In this work, we compile a global map of deltas and propose an updated catalog (https://doi.org/10.6084/m9.figshare.14564319) that includes previous confirmed observations and new detections. We especially report geomorphological traits, investigate the temporal and spatial relationships among the deposits, and

compare them to the surrounding environment, to assess the relevance and potential of deltas for the reconstruction of past climate conditions on Mars.

2. Data and Methods

For the morphologic interpretations, we used a Context Camera (CTX; ~6 m/pixel) global mosaic (Dickson et al., 2018; Malin et al., 2007) while the topographic information was derived from the MOLA (~460 m/pixel; Smith et al., 2001; Zuber et al., 1992) colorized elevation model to have an informative global coverage at the highest resolution available. For localized elevation data, where available, we also relied on HRSC Digital Elevation Models providing a vertical resolution of ~12 m and a regular grid spacing of 50–100 m (Gwinner et al., 2016; Scholten et al., 2005). Observations, mapping, and measurements were made using the QGis software, while for age determination we used the crater size-frequency distributions of impact craters (Hartmann & Neukum, 2001).

We used geomorphological characteristics to perform a global search and mapping of deltas across the Martian surface. Depositional features were interpreted as delta fans when they appeared as fan-shaped deposits fed by a channel, characterized by either a stack of steep foresets of decreasing radius, or by a single steep foreset, either flat-topped or branched (De Villiers et al., 2009, 2013; Hauber et al., 2013). Through the identification of these characterizing traits, delta fans were distinguished from alluvial fans visually and through the generation of DEM-derived cross sections. In fact, alluvial fans are defined, differently from deltas, as gently sloping semi-conical landforms associated with the discharge of water and sediments from a confined channel into an unconfined terrain characterized by the absence of a standing body of water (e.g., Moore & Howard, 2005; Morgan et al., 2014). For each observed delta, we collected the following data:

(1) location coordinates,
(2) a mean elevation value of the deposit's front (i.e., the upper slope break of the frontal scarp).
(3) length and type of the feeding channel (Alemanno et al., 2018),
(4) type of basin, which hosts the delta: closed basin = craters with intact rims; lake with outlet = confined low-lying regions with both inlet valleys and an outlet valley (craters with breached rimes, Goudge et al., 2012); and open basin = deltas not contained within craters or deltas formed at the mouth of tributaries opening into outflow channels (Di Achille & Hynek, 2010),
(5) flow direction (derived by measuring the direction that connects the apex to the front of the delta),
(6) delta morphology categorized with relation to the basin water level according to De Villiers et al., (2013): stepped delta (water level rising); prograding delta (water level constant); and incised/telescoping delta (water level dropping).

3. Observations

Across the whole planet, we identified a global population of 161 deltas (Figure 1a), among which 68 were not reported in previous catalogs that provided delta locations (Di Achille & Hynek, 2010; Fassett and Head, 2007, 2008; Hauber et al., 2013; Irwin et al., 2015; Palucis et al., 2016; Wilson et al., 2021). The elevation range where these deposits are found spans from a minimum of −4,950 m to a maximum of 2,889 m with a mean elevation value of −1,623 m and a median value of −1,933 m. The overall elevation distribution displays a peak abundance of deltas between about −1,900 and −2,700 m that includes around one third of the whole population (Figure 1b).

Both deltas, channels, and open-lake basin populations are predominantly abundant between 60°S and 30°N (Alemanno et al., 2018; Fassett & Head, 2008). According to the channel length distribution (Alemanno et al., 2018), deltas are mostly located at the tip of channels shorter than 30 km and quickly diminish in frequency at growing lengths (Figure 1c). The length of the feeding channel connected to the presence of a delta deposit has been suggested to be: (a) a possible proxy for the duration of the aqueous activity in the channel-delta system and (b) proportional to the age of the delta (Hauber et al., 2013). Short channel lengths are usually associated with pristine morphologies and the absence of mineral alteration suggesting short-lived aqueous processes, specifically, the latter relationship links older deltas near Chryse Planitia (>3 Ga) to longer valleys, while younger deltas are usually fed by shorter valleys (Hauber et al., 2013).

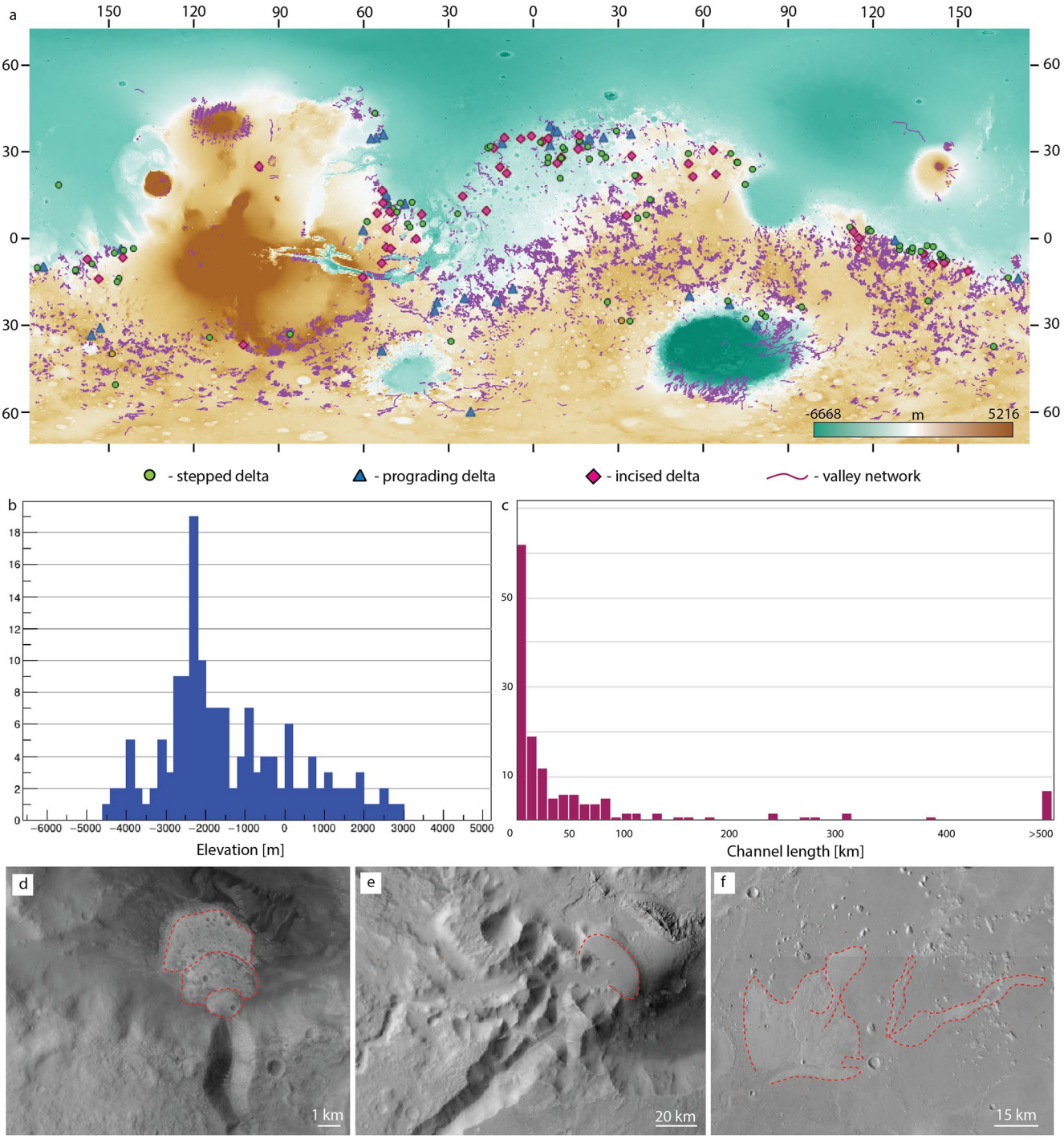

Figure 1. (a) The herein proposed delta population is plotted on a MOLA colorized elevation model and the valley network (Alemanno et al., 2018). Each delta location is classified according to the three main morphologies identified as a function of the water level behavior. Delta frequency (*y* axis) versus the delta front elevation (*x* axis) is shown in panel b, while delta frequency (*y* axis) versus the feeding channel length (*x* axis) is presented in panel (c) Examples of the different morphological classes are shown in panels (d)–(f): stepped delta (d), prograding delta (e), and incised delta (f).

These relationships might be explained by the decreasing availability of liquid water with time in a growing cryosphere, where older deltas formed in a relatively warmer environment when water could be derived over longer time spans or across spatially more extended source regions, both leading to larger and longer feeding valleys (Hauber et al., 2013). The global overview on delta deposits thus highlights that a large

portion of the delta population have the potential to be quite young (Hauber et al., 2013). This constitutes a critical aspect that needs to be considered in the future in order to draw further conclusions concerning water availability throughout Martian history.

The previous global delta catalog from Di Achille and Hynek (2010) classified deltas based on the type of basin where the deposit is found. In order to create a comparable updated data set, we used their classification of closed and open basins to distinguish deltas enclosed into craters or not. We additionally highlighted deltas contained in craters with breached rims by separating them into an extra class that we characterized according to the definition of an open basin lake by Goudge et al. (2012). Across our inventory, we found 120 deltas enclosed within endorheic (craters, i.e., closed basins) or exorheic (lake with outlet) basins, while only 41 are hosted within the outflow channel networks or directly within the northern plains (open basins class). On Mars, the delta morphology is primarily affected by the water level behavior. We updated the delta catalog by classifying each deposit based on its morphology: stepped or retrograding deltas formed during water level rise; prograding deltas representing constant water level; and incised deltas, partially destroyed by erosion, indicating water level fall (De Villiers et al., 2013). However, along with water level behavior, sediment supply also plays a role in the definition of delta morphologies. De Villiers et al. (2013) conducted experiments with a fluctuating sediment supply to simulate a real case scenario (e.g., initial collapse of the upstream crater rim and decreasing bank erosion due to feeder channel widening and diminishing flow velocity). On Mars, sediment fluctuation is unknown, and thus, some degree of uncertainty remains especially for: prograding deltas that might also form during water level rise when an adequate sediment supply is present; and in large basins, where water level fluctuation may be very slow compared to the small basin scenario used in the experiments. We assigned each delta to a morphological class, which is linked to the most recent water level change recorded by the deposit and detected 47 stepped deltas, 82 prograding deltas, and 32 incised deltas. By coupling the morphological and the basin classifications, we find that all stepped deltas are found enclosed in endorheic basins with the only exception of five cases where the deltas are located into craters with breached rims. Conversely, all incised deltas are located in open basins or lakes with an outlet counting only four exceptions that can be found in closed basins. We investigated the feeding channel length and elevation distributions for these three morphology-based subgroups but found no significant deviation from the global trends. We also measured the orientation of deltas and found no preferential trends, which is different from what was previously reported by Morgan et al. (2018), who observed for stepped deltas and alluvial fans, a prominent N-S trend that they interpreted as an indicator of control by solar insolation. Since no alluvial fans were included in the present work, it might be hypothesized that the recorded trend was mainly ascribable to alluvial fans instead of deltas.

4. Discussions

Widespread evidence points to the possible existence of an ancient Martian ocean (e.g., Baker et al., 1991; Carr & Head, 2003; Clifford & Parker, 2001; Head et al., 1999; Parker et al., 1989, 1993), and deltas have been discussed as possible proxies to reconstruct the paleo water level (Di Achille & Hynek, 2010; Horvath & Andrews-Hanna, 2017; Rivera-Hernández & Palucis, 2019). We test the likelihood of a northern Martian ocean hypothesis by examining the global-scale overview on the topography and distribution of the delta population.

We first selected a subpopulation of deltas located at the margin of the northern plains without any evident topographical barrier. Thus, we kept only deposits that might have formed at the edge of the same large ocean-like water body. By performing this downselection, we reduced the population to 29 deltas (Figure 2a). All of the identified deltas are located along the dichotomy boundary between 15°S and 45°N with an elevation range between −3,941 and −933 m (mean = −2,318 m; median = −2,306 m; mode = −2,440 m). We always refer to the entire elevation range since the topographical distribution of the deposits is never statistically a normal distribution; hence, providing just typical statistical values such as mean and standard deviations lead to the omission of meaningful data (cf., Figure S1). If this subgroup of deltas was associated with the same water body that putatively occupied the northern hemisphere, the topography around the deposits should progressively descend toward the lowlands (mostly in the north) devoid of topographical obstructions. We thus carried out a local-scale analysis of the elevation trend at each delta location investigating the surrounding environment up to a distance from the delta where obstructing morphologies were

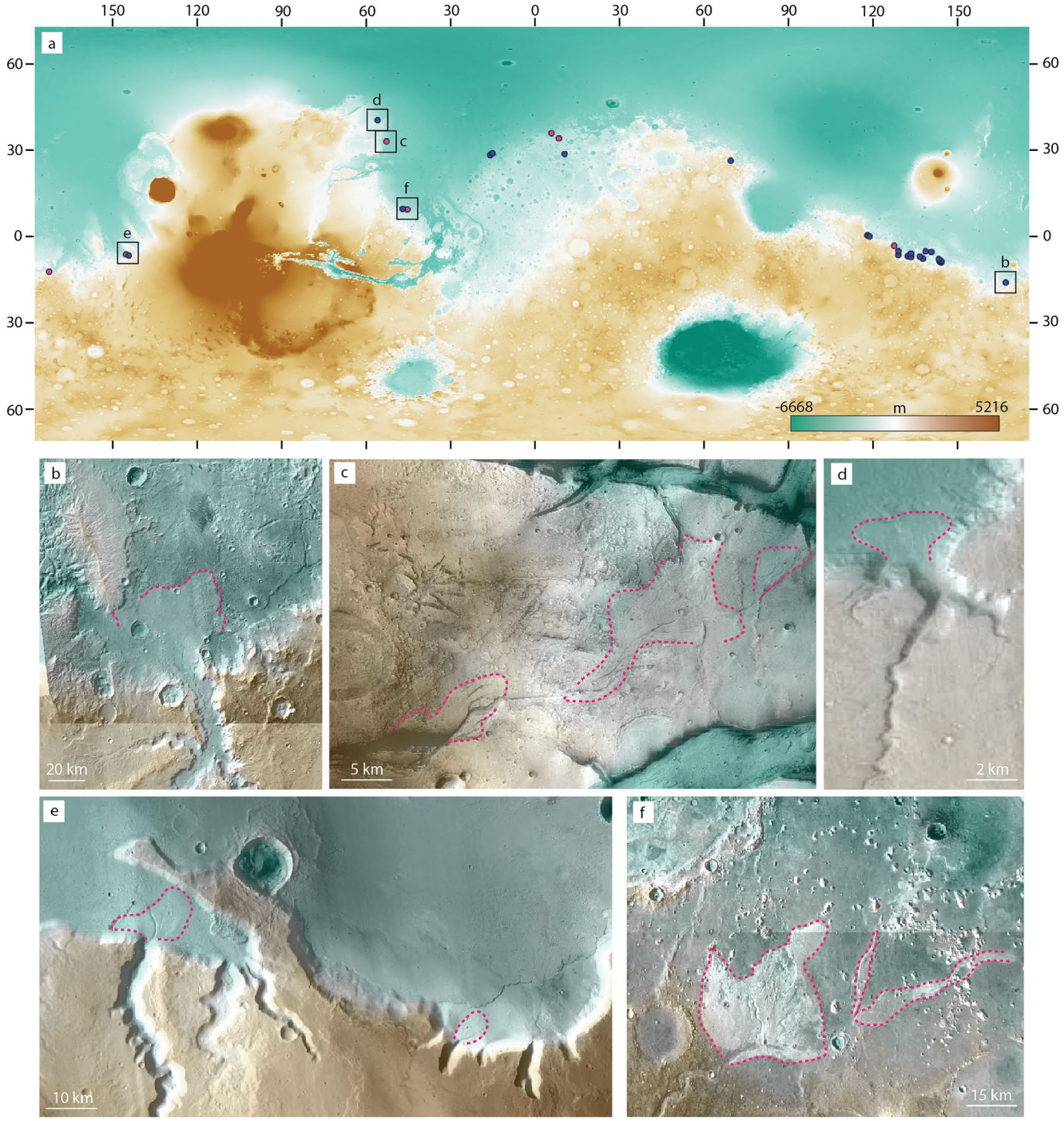

Figure 2. (a) Locations of the 29 selected deltas not enclosed in closed basins, lakes with outlets, or located within outflow channels are displayed according to their morphological trait classification (see caption Figure 1). The six deltas that are also not associated with local topographic depressions are framed in panel (a) on a global scale and displayed at higher resolution below (CTX global mosaic; Malin et al., 2007): (b) de Vaucouleurs Crater delta; (c) Chryse Planitia delta located at 36°N–52°W; (d) Acidalia Planitia delta located at 44°N–56°W; (e) Memnonia deltas; and (f) Hypanis Valles fan-shaped deposit.

present. The analysis was concluded when the contour lines showed a consistent progressive topographical smooth decrease toward the north. Through this analysis, we observed that 23 out of 29 deltas are enclosed in topographic depressions. Additionally, the elevation of these basins' rims often coincides with the elevation of the included delta front. Accordingly, there is no evidence that precludes the possibility that such depressions might have acted as local ponds at the time of delta formation. Although it cannot be excluded,

no presence of a standing body of water extending across the northern plains is required to explain the existence of these deltas. Only six deltas, hence, appear to have had the potential to be located directly at the margin of a northern ocean. Nevertheless, the widespread presence of deltas across the Martian surface, and thus of hosting water-filled basins, suggests that the water input, both from the surface and the subsurface, must have exceeded evaporation and infiltration leading the basins to fill and be stable enough to allow the generation of deltas at the inlet mouth. Especially, the mere presence of deltas that are not hosted in local topographic depressions but linked to the large basin that might have possibly hosted an ancient ocean suggests that at some point the Martian climatic conditions could have sustained a significantly extended body of water. For this to happen, it might be necessary to invoke the presence of a global water cycle, including a groundwater flow, which might also have reached the surface in low elevated areas, as for example, in the northern lowlands (Fassett & Head, 2008).

Despite the fact that closed basins in proximity to an ocean shoreline may present some subsurface hydrological connection to the ocean and thus display a similar water level, the uncertainties in the selection of this further subgroup of deltas are too large to avoid an arbitrary sampling. Hence, we only investigated the six deltas that, from the observation of the present-day topography, appear not to be enclosed into craters or other topographic depressions, and thus, have higher probabilities to have formed at the margin of an ancient Martian ocean.

(1) Hypanis Valles delta: the Hypanis delta is a complex deposit located at 11°N–45°W that recorded several water-level stages between about −2,500 and −3,000 m on a period spanning from the Late Noachian to the Early Hesperian (for an extensive description refer to Fawdon et al., 2018; Figure 2f)

(2) de Vaucouleurs Crater delta: this is a highly degraded deposit located at 15°S–171°E (Figure 2b). The feeding channel cuts a Middle Noachian unit and terminates on a Hesperian and Noachian Transition unit (Parker et al., 2010; Tanaka et al., 2014). The de Vaucouleurs crater rims are still visible on the southwestern side, but the whole crater appears to be pervasively affected, or completely disrupted, by younger chaos terrain formation that degraded also the delta deposit. The delta front today is located at −1,700 m, but due to the chaos formation it cannot be excluded that the front might have been displaced or eroded up to the present-day configuration. The current topography shows no barrier between the delta and the northern plains, nevertheless, it needs to be acknowledged that there is no evidence precluding the possibility that the delta formation took place mainly before the chaos formation, while water was more likely to be contained within the crater rims.

(3) Chryse Planitia delta: This delta (Figure 2c) is located at 36°N–52°W and displays multiple incised fans from an elevation of about −3,100 m to −3,280 m. The delta activity is likely to have lasted during a period between the Late Noachian and the Early Hesperian; in fact, the latest unit that the channel-delta system cut is dated Late Noachian (Tanaka et al., 2014), while the delta tip appears to be cut by a system of grabens, which on an area slightly to the south, are estimated to be around Early Hesperian in age (Nouvel et al., 2006). Nonetheless, age estimates performed on this channel network suggest this terminal area to be 2.43 Ga old (Salese et al., 2016). Due to the presence of faults, it must be taken into account that a certain extent of displacement from its original topographical location might have occurred.

(4) Acidalia Planitia delta: This deposit (Figure 2d) is located 480 km north from the Chryse planitia delta at 44°N–56°W. It is a prograding delta located at −2,203 m on a Middle Noachian unit (Tanaka et al., 2014).

(5) Memnonia deltas: at this location two deltas are found at the boundary between the same two units at around 50 km apart (Figure 2e). Besides being spatially extremely close (~ 5°S–147°W), these two features display similar characteristics, and the delta fronts are located at about (a) −2,525 m and (b) −2,306 m, respectively. One of the two deposits appears to be of outstanding relevance since part of the delta fan is covered by a younger unit that allows us to determine both a minimum and a maximum age for this delta. According to the global Martian map of Tanaka et al. (2014), the unit cut by the feeding channel, thus older than the delta formation, belongs to the Amazonian and Hesperian Volcanic units (AHv) while the one deposited on top of the delta is estimated to be a Late Hesperian transition unit (lHt). For a higher degree of detail, we performed CTX-derived impact crater statistic (chronology functions: Michael, 2013 and Hartmann & Neukum, 2001; production function: Ivanov et al., 2001) on the

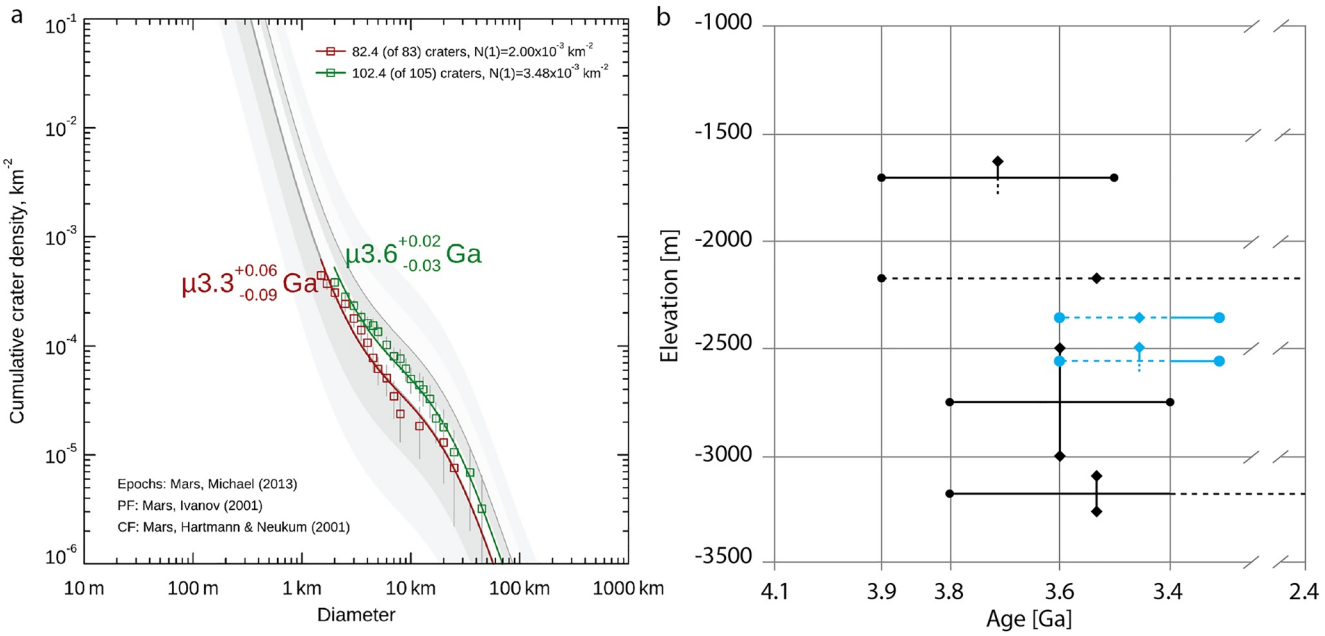

Figure 3. (a) Impact crater cumulative size frequency distribution plots with fitted model ages for the Late Hesperian transition unit (red plot) and the Amazonian and Hesperian Volcanic unit (green plot). (b) Elevation of the delta fronts are plotted against the estimated time span during potential delta activity. Limit values for elevation and time are indicated with diamond and circle symbols, respectively. If the limit values are unknown or uncertain dashed lines and/or no symbol are displayed. Age determinations in panel a refer to the Memnonia deltas displayed in blue in panel (b).

underlying and overlapping units on 445 and 339 craters on areas of 2.7×10^6 km^2 and 1.8×10^6 km^2, respectively, constraining the delta emplacement between 3.6 and 3.3 Ga (Figure 3a). We estimate that this time interval accounts for both the Memnonia deltas. Our observations suggest that the two deltaic deposits correspond to two stages of water level drop within the same basin. The two deltas in this area display channel incision on the delta plain and can be classified as prograding or incised deltas (uncertainties are due to the partial obliteration) thus excluding the hypothesis of a water level rise. This portion of the basin is elongated and deepens moving from SE toward NW and finally opens toward the northern plains without showing any interposed barrier on the present-day topography. The elevations of the two delta fronts approximate two levels of well visible terraces and filled coves along the basin boundary suggesting a progressive water level drop pushing the coastline northwestward until the runoff from the highlands stopped. In fact, no evidence of channels or fluvial activity is recorded on the lHt unit that filled the basin around 3.3 billion years ago (cf., Figure S2).

To test the hypothesis that these deltas once developed at the margin of the same ocean-like water body, we compared the elevation range and formation time (Figure 3b). If an ocean ever occupied the northern regions of Mars, after its optimum, it must have progressively retreated up to a degree of depletion compatible with the present-day situation. Indeed, two subsequent extensive shoreline contacts, Arabia and Deuteronilus, have been observed (Clifford & Parker, 2001; Perron et al., 2007) and their evolution has been analyzed taking into consideration the topographical displacement that likely occurred during the Tharsis emplacement (Citron et al., 2018) and related isostatic rebound (Citron et al., 2021). Shorelines' location and reliability remain, however, controversial. Hypothesized shoreline maps published through time (Carr & Head, 2003; Clifford & Parker, 2001; Ivanov et al., 2017; Parker et al., 1989, 1993; Perron et al., 2007; Webb, 2004) show inconsistencies and wide displacements, especially concerning the Arabia shoreline reconstruction; hence, caution needs to be taken in using these data and drawing conclusions about the Martian climate history (Sholes et al., 2021). Overall, the Arabia shoreline is suggested to have formed shortly after the early Tharsis formation around 4 Gyr ago (Citron et al., 2018; Clifford & Parker, 2001), while the younger Deuteronilus shoreline is dated about 3.6 Gyr ago (Ivanov et al., 2017) after most of the Tharsis province was emplaced. What role the Tharsis emplacement played in the climatic and topographical evolution is still debated (e.g., Bouley et al., 2016; Halevy & Head, 2014; Tian et al., 2010; Wordsworth et al., 2015).

Therefore, we did not rely on any specific scenario and used present-day topography for the analyses, since the Martian water drainage is dominated by local or regional slopes rather than by large-scale elevations (Irwin et al., 2011). Nonetheless, whether a standing body of water occupied the northern plains, deltas should have then recorded the shoreline repositioning through time. Thus, expected water level fluctuations might have led to continuous delta formation and erosion up to a final stage of retreat that led to the present-day waterless condition. This latest phase has accordingly the highest chances to be preserved in the geological record, hence expecting younger deltas to be found at progressively lower elevations. However, no age-elevation correlation among our six deltas can be conclusively identified due to the large time spans of potential delta activity (Figure 3b). To further test this hypothesis, we also compared deltas and shoreline positions at each delta site since a certain degree of agreement would be expected. With the only exception of the de Vaucouleurs crater delta, which matches the Arabia shoreline position and timing, the other delta deposits show discrepancies. The Memnonia deltas represent a good example highlighting clear contradiction between the two data sets. We constrained the Memnonia deltas' formation between 3.6 and 3.3 Gyr ago, thus expecting at least partial matching with the coeval or even slightly older Deuteronilus shoreline location. Differently, the Memnonia delta location is better represented by the Arabia shoreline, which is, however, dated early Noachian, while the Deuteronilus shoreline appears to sit several latitudinal degrees northward (Citron et al., 2018 and references therein). Nonetheless, from the analysis of knickpoints in Martian channels in this area, it has been suggested that the Arabia shoreline was reoccupied by the ocean coastline during the late Hesperian due to a significant water level rise that might have occurred between 3.6 and 3.4 Ga (Duran et al., 2019). This interpretation of the ocean evolution shows a good agreement with the observed delta location and age we report, but may collide with the morphology of Memnonia deltas, which seems to indicate water level decrease. Nevertheless, these potential contradictory observations can be reconciled hypothesizing that these deltas represent the result of a further water drop occurring between 3.4 Ga (Duran et al., 2019) and 3.3 Ga (lHt unit age), which necessarily must have followed the water level rise to reach the present-day conditions. Despite that, within the population of candidate delta fans documented in this study, we systematically find stepped deltas (i.e., the delta morphology associated with a rising water level) exclusively associated with closed basins suggesting either unfavorable conditions for the formation of this kind of morphology, a complete global obliteration of these features in association with the northern sea level rise or a progressive continuous drop in the ocean level.

5. Conclusions

The global inventory of deltas presented herein aims to provide a large-scale overview on the delta deposit distribution and characteristics. We seek to identify the relationship between these features and a hypothesized ancient northern ocean. Accordingly, we focused on those deposits marginally to the basin that would have hosted a northern ocean (29 deltas out of 161). However, only six of them have a high potential of being representative of an oceanic paleo-shoreline. These six deltas are located at different elevations, but no spatial-temporal relationship could be found between their elevations and the time intervals when they had the potential to be active, as would have been expected if they followed a consistently rising or falling water level. Hence, delta information is insufficient to determine a global water level behavior. We looked for similarities in timing and distribution among deltas and shorelines to investigate potential connections. However, we revealed discrepancies between these two data sets making it hard to fully reconcile previously adopted interpretations to the currently analyzed landforms.

Overall, there is no compelling evidence that would make deltas alone a constraining proxy for a global oceanic water level reconstruction on Mars, as previously suggested. Deltas cannot be considered sufficient evidence to identify one shoreline or a consistent shoreline evolution trend, but they may be representative of shoreline fluctuation over time if they develop at the margin of the same body of water. This result challenges the paradigm of the single global water level perspective derived from the previous delta analysis on a planet scale (Di Achille & Hynek, 2010). More modeling and observations are needed to tackle and explain the discrepancy observed in this study between delta deposits and proposed shorelines. A reconciling interpretation might in fact provide further clues and constraints for the Martian climatic evolution.

Data Availability Statement

Data sets produced for this research are included as supporting information at: https://doi.org/10.6084/m9.figshare.14564319.v1.

Acknowledgments
We thank two anonymous reviewers for their thoughtful comments that helped to improve an earlier version of this paper. We also thank the editor Andrew J. Dombard for handling this manuscript. B. De Toffoli and A.-C. Plesa gratefully acknowledge the financial support and endorsement from the DLR Management Board Young Research Group Leader Program and the Executive Board Member for Space Research and Technology. Open access funding enabled and organized by Projekt DEAL.

References

Alemanno, G., Orofino, V., & Mancarella, F. (2018). Global map of Martian fluvial systems: Age and total eroded volume estimations. *Earth and Space Science*, *5*, 560–577. https://doi.org/10.1029/2018EA00036

Baker, V. R., Strom, R. G., Gulick, V. C., Kargel, J. S., & Komatsu, G. (1991). Ancient oceans, ice sheets and the hydrological cycle on Mars. *Nature*, *352*, 584–589. https://doi.org/10.1038/352589a0

Bouley, S., Baratoux, D., Matsuyama, I., Forget, F., Séjourné, A., Turbet, M., & Costard, F. (2016). Late Tharsis formation and implications for early Mars. *Nature*, *531*, 344–347. https://doi.org/10.1038/nature1717

Carr, M. H., & Head, J. W. (2003). Oceans on Mars: An assessment of the observational evidence and possible fate. *Journal of Geophysical Research: Solid Earth and Planets*, *108*, 5042. https://doi.org/10.1029/2002je001963

Carr, M. H., & Head, J. W. (2015). Martian surface/near-surface water inventory: Sources, sinks, and changes with time. *Geophysical Research Letters*, *42*, 726–732. https://doi.org/10.1002/2014gl062464

Citron, R. I., Manga, M., & Hemingway, D. J. (2018). Timing of oceans on Mars from shoreline deformation. *Nature*, *555*, 643–646. https://doi.org/10.1038/nature26144

Citron, R. I., Manga, M., Hemingway, D. J., & Plattner, A. (2021). *Are we visiting the coastlines of Mars? Load-Corrected Paleo-ocean levels At Jezero, Oxia Planum,Andgale*. Lunar and Planetary Science Conference.

Clifford, S. M., & Parker, T. J. (2001). The evolution of the Martian hydrosphere: Implications for the fate of a primordial ocean and the current state of the Northern Plains. *Icarus*, *154*, 40–79. https://doi.org/10.1006/icar.2001.6671

De Villiers, G., Kleinhans, M. G., & Postma, G. (2013). Experimental delta formation in crater lakes and implications for interpretation of Martian deltas. *Journal of Geophysical Research: Solid Earth and Planets*, *118*, 651–670. https://doi.org/10.1002/jgre.20069

De Villiers, G., Kleinhans, M. G., Postma, G., Hauber, E., de Jong, S., & de Boer, P. L. (2009). Types of Martian fan-shaped sedimentary deposits. *Lunar and Planetary Science Conference*, *40*, 1901.

Di Achille, G., & Hynek, B. M. (2010). Ancient Ocean on Mars supported by global distribution of deltas and valleys. *Nature Geoscience*, *3*, 459–463. https://doi.org/10.1038/ngeo891

Di Biase, R. A., Limaye, A. B., Scheingross, J. S., Fischer, W. W., & Lamb, M. P. (2013). Deltaic deposits at Aeolis Dorsa: Sedimentary evidence for a standing body of water on the northern plains of Mars. *Journal of Geophysical Research: Solid Earth and Planets*, *118*, 1285-–1302. https://doi.org/10.1002/jgre.20100

Dickson, J. L., Kerber, L., Fassett, C. I., & Ehlmann, B. L. (2018). *A global, blended Ctx mosaic of mars with vectorized seam mapping: A new mosaicking pipeline using principles of non-destructive image editing*. Lunar and Planetary Science Conference.

Duran, S., Coulthard, T. J., & Baynes, E. R. C. (2019). Knickpoints in Martian channels indicate past ocean levels. *Scientific Reports*, *9*, 1–6. https://doi.org/10.1038/s41598-019-51574-2

Fassett, C. I., & Head, J. W. (2007). Valley formation on martian volcanoes in the Hesperian: Evidence for melting of summit snowpack, caldera lake formation, drainage and erosion on Ceraunius Tholus. *Icarus*, *189*, 118–135. https://doi.org/10.1016/j.icarus.2006.12.021

Fassett, C. I., & Head, J. W. (2008). Valley network-fed, open-basin lakes on Mars: Distribution and implications for Noachian surface and subsurface hydrology. *Icarus*, *198*, 37–56. https://doi.org/10.1016/j.icarus.2008.06.016

Fawdon, P., Gupta, S., Davis, J. M., Warner, N. H., Adler, J. B., Balme, M. R., et al. (2018). The Hypanis Valles delta: The last highstand of a sea on early Mars? *Earth and Planetary Science Letters*, *500*, 225–241. https://doi.org/10.1016/j.epsl.2018.07.040

Goudge, T. A., Head, J. W., Mustard, J. F., & Fassett, C. I. (2012). An analysis of open-basin lake deposits on Mars: Evidence for the nature of associated lacustrine deposits and post-lacustrine modification processes. *Icarus*, *219*, 211–229. https://doi.org/10.1016/j.icarus.2012.02.027

Goudge, T. A., Milliken, R. E., Head, J. W., Mustard, J. F., & Fassett, C. I. (2017). Sedimentological evidence for a deltaic origin of the western fan deposit in Jezero crater, Mars and implications for future exploration. *Earth and Planetary Science Letters*, *458*, 357–365. https://doi.org/10.1016/j.epsl.2016.10.056

Gwinner, K., Jaumann, R., Hauber, E., Hoffmann, H., Heipke, C., Oberst, J., et al. (2016). The High Resolution Stereo Camera (HRSC) of Mars Express and its approach to science analysis and mapping for Mars and its satellites. *Planetary and Space Science*, *126*, 93–138. https://doi.org/10.1016/j.pss.2016.02.014

Halevy, I., & Head, J. W. (2014). Episodic warming of early Mars by punctuated volcanism. *Nature Geoscience*, *7*, 865–868. https://doi.org/10.1038/ngeo2293

Hartmann, W. K., & Neukum, G. (2001). Cratering chronology and the evolution of Mars. *Space Science Reviews*, *96*, 165–194. https://doi.org/10.1007/978-94-017-1035-0_6

Hauber, E., Platz, T., Reiss, D., Le Deit, L., Kleinhans, M. G., Marra, W. A., et al. (2013). Asynchronous formation of Hesperian and Amazonian-aged deltas on Mars and implications for climate. *Journal of Geophysical Research: Solid Earth and Planets*, *118*, 1529–1544. https://doi.org/10.1002/jgre.20107

Head, J. W., Hiesinger, H., Ivanov, M. A., Kreslavsky, M. A., Pratt, S., & Thomson, B. J. (1999). Possible ancient oceans on Mars: Evidence from Mars Orbiter Laser Altimeter data. *Science*, *286*, 2134–2137. https://doi.org/10.1126/science.286.5447.2134

Horvath, D. G., & Andrews-Hanna, J. C. (2017). Reconstructing the past climate at Gale crater, Mars, from hydrological modeling of late-stage lakes. *Geophysical Research Letters*, *44*, 8196–8204. https://doi.org/10.1002/2017GL074654

Hynek, B. M., Hoke, M. R. T., & Beach, M. (2010). Updated global map of Martian valley networks and implications for climate and hydrologic processes. *Journal of Geophysical Research*, *115*, E09008. https://doi.org/10.1029/2009JE003548

Irwin, R. P., Craddock, R. A., Howard, A. D., & Flemming, H. L. (2011). Topographic influences on development of Martian valley networks. *Journal of Geophysical Research*, *116*, E02005. https://doi.org/10.1029/2010je003620

Irwin, R. P., Lewis, K. W., Howard, A. D., & Grant, J. A. (2015). Paleohydrology of Eberswalde crater, Mars. *Geomorphology*, *240*, 83–101. https://doi.org/10.1016/j.geomorph.2014.10.012

Ivanov, B., Neukum, G., & Wagner, R. (2001). Size-frequency distributions of planetary impact craters and asteroids. In *Collisional processes in the solar system* (pp. 1–34). Springer. https://doi.org/10.1007/978-94-010-0712-2_1

Ivanov, M. A., Erkeling, G., Hiesinger, H., Bernhardt, H., & Reiss, D. (2017). Topography of the Deuteronilus contact on Mars: Evidence for an ancient water/mud ocean and long-wavelength topographic readjustments. *Planetary and Space Science*, *144*, 49–70. https://doi.org/10.1016/j.pss.2017.05.012

Malin, M. C., Bell, J. F., Cantor, B. A., Caplinger, M. A., Calvin, W. M., Clancy, R. T., et al. (2007). Context camera investigation on board the Mars Reconnaissance Orbiter. *Journal of Geophysical Research*, *112*, E05S04. https://doi.org/10.1029/2006JE002808

Mangold, N., Dromart, G., Ansan, V., Salese, F., Kleinhans, M. G., Massé, M., et al. (2020). Fluvial regimes, morphometry, and age of Jezero Crater Paleolake Inlet Valleys and their exobiological significance for the 2020 rover mission landing site. *Astrobiology*, *20*, 994–1013. https://doi.org/10.1089/ast.2019.2132

Michael, G. G. (2013). Planetary surface dating from crater size–frequency distribution measurements: Multiple resurfacing episodes and differential isochron fitting. *Icarus*, *226*, 885–890. https://doi.org/10.1016/j.icarus.2013.07.004

Moore, J. M., & Howard, A. D. (2005). Large alluvial fans on Mars. *Journal of Geophysical Research*, *110*, E04005. https://doi.org/10.1029/2004JE002352

Morgan, A. M., Howard, A. D., Hobley, D. E., Moore, J. M., Dietrich, W. E., Williams, R. M. E., et al. (2014). Sedimentology and climatic environment of alluvial fans in the Martian Saheki crater and a comparison with terrestrial fans in the Atacama Desert. *Icarus*, *229*, 131–156. https://doi.org/10.1016/j.icarus.2013.11.007

Morgan, A. M., Wilson, S. A., Howard, A. D., Craddock, R. A., & Grant, J. A. (2018). Global Distribution of Alluvial Fans And Deltas On Mars. Lunar Planet. Sci. Conf. Contrib. No. 2083. https://doi.org/10.1130/abs/2018am-317138

Nazari-Sharabian, M., Aghababaei, M., Karakouzian, M., & Karami, M. (2020). Water on Mars-A literature review. *Galaxies*, *8*, 40. https://doi.org/10.3390/GALAXIES8020040

Nouvel, J.-F., Martelat, J.-E., Herique, A., & Kofman, W. (2006). Top layers characterization of the Martian surface: Permitivity estimation based on geomorphology analysis, *Planetary and Space Science*, *54*, 337–344. https://doi.org/10.1016/j.pss.2005.12.013

Ori, G. G., Marinangeli, L., & Baliva, A. (2000). Terraces and gilbert-type deltas in crater lakes in Ismenius lacus and Memnonia (Mars). *Journal of Geophysical Research*, *105*, 17629–17641. https://doi.org/10.1029/1999je001219

Palucis, M., Dietrich, W. E., Williams, R. M. E., Hayes, A. G., Parker, T., Sumner, D. Y., et al. (2016). Sequence and relative timing of large lakes in Gale crater (Mars) after the formation of Mt. Sharp. *Journal of Geophysical Research: Solid Earth and Planets*, *121*, 472–496. https://doi.org/10.1002/2015JE004905

Parker, M. V. K., Zegers, T., Kneissl, T., Ivanov, B., Foing, B., & Neukum, G. (2010). 3D structure of the Gusev Crater region. *Earth and Planetary Science Letters*, *294*(3–4), 411–423. https://doi.org/10.1016/j.epsl.2010.01.013

Parker, T. J., Gorsline, D. S., Saunders, R. S., Pieri, D. C., & Schneeberger, D. M. (1993). Coastal geomorphology of the Martian northern plains. *Journal of Geophysical Research*, *98*, 11061–11078. https://doi.org/10.1029/93je00618

Parker, T. J., Saunders, S. R., & Schneeberger, D. M. (1989). Transitional morphology in West Deuteronilus Mensae, Mars: Implications for modification of the lowland/upland boundary. *Icarus*, *82*(1), 111–145. https://doi.org/10.1016/0019-1035(89)90027-4

Perron, J. T., Mitrovica, J. X., Manga, M., Matsuyama, I., & Richards, M. A. (2007). Evidence for an ancient Martian ocean in the topography of deformed shorelines. *Nature*, *447*, 840–843. https://doi.org/10.1038/nature05873

Rivera-Hernández, F., & Palucis, M. C. (2019). Do deltas along the crustal dichotomy boundary of Mars in the Gale crater region record a Northern ocean? *Geophysical Research Letters*, *46*, 8689–8699. https://doi.org/10.1029/2019GL083046

Salese, F., Di Achille, G., Neesemann, A., Ori, G. G., & Hauber, E. (2016). Hydrological and sedimentary analyses of well-preserved paleo-fluvial-paleolacustrine systems at Moa Valles, Mars. *Journal of Geophysical Research: Solid Earth and Planets*, *121*, 194–232. https://doi.org/10.1002/2015JE004891

Scholten, F., Gwinner, K., Roatsch, T., Matz, K.-D., Wählisch, M., Giese, B., et al. (2005). Mars express HRSC data processing—Methods and operational aspects. *Photogrammetric Engineering & Remote Sensing*, *71*, 1143–1152. https://doi.org/10.14358/pers.71.10.1143

Sholes, S., Dickeson, Z., Montgomery, D., & Catling, D. (2021). Data For: Where are Mars' hypothesized ocean shorelines? Large lateral and topographic offsets between different versions of Paleoshoreline maps. *Journal of Geophysical Research: Solid Earth and Planets*, *126*. https://doi.org/10.1029/2020JE006486

Smith, D. E., Zuber, M. T., Frey, H. V., Garvin, J. B., Head, J. W., Muhleman, D. O., et al. (2001). Mars orbiter laser altimeter: Experiment summary after the first year of global mapping of Mars. *Journal of Geophysical Research*, *106*, 23689–23722. https://doi.org/10.1029/2000je001364

Summons, R. E., Amend, J. P., Bish, D., Buick, R., Cody, G. D., Des Marais, D. J., et al. (2010). *Preservation of Martian organic and environmental records*. Posted April, 2010, by the Mars Exploration Program Analysis Group (MEPAG). Retrieved from http://mepag.jpl.nasa.gov/reports/

Tanaka, K. L., Robbins, S. J., Fortezzo, C. M., Skinner, J. A., & Hare, T. M. (2014). The digital global geologic map of Mars: Chronostratigraphic ages, topographic and crater morphologic characteristics, and updated resurfacing history. *Planetary and Space Science*, *95*, 11–24. https://doi.org/10.1016/j.pss.2013.03.006

Tian, F., Claire, M. W., Haqq-Misra, J. D., Smith, M., Crisp, D. C., Catling, D., & Kasting, J. F. (2010). Photochemical and climate consequences of sulfur outgassing on early Mars. *Earth and Planetary Science Letters*, *295*(3–4), 412–418. https://doi.org/10.1016/j.epsl.2010.04.016

Webb, V. E. (2004). Putative shorelines in northern Arabia Terra, Mars. *Journal of Geophysical Research: Planets*, *109*, E09010. https://doi.org/10.1029/2003JE002205

Wilson, S. A., Morgan, A. M., Howard, A. D., & Grant, J. A. (2021). The Global distribution of craters with alluvial fans and deltas on Mars. *Geophysical Research Letters*, *48*. https://doi.org/10.1029/2020gl091653

Wordsworth, R. D., Kerber, L., Pierrehumbert, R. T., Forget, F., & Head, J. W. (2015). Comparison of "warm and wet" and "cold and icy" scenarios for early Mars in a 3-D climate model: Warm and wet vs. cold and icy early Mars. *Journal of Geophysical Research: Solid Earth and Planets*, *120*, 1201–1219. https://doi.org/10.1002/2015je004787

Zuber, M. T., Smith, D. E., Solomon, S. C., Muhleman, D. O., Head, J. W., Garvin, J. B., et al. (1992). The Mars observer laser altimeter investigation. *Journal of Geophysical Research*, *97*, 7781–7797. https://doi.org/10.1029/92JE00341